Journal of Alloys and Compounds 525 (2012) 149–153

Contents lists available at SciVerse ScienceDirect

Journal of Alloys and Compounds

journal homepage: www.elsevier.com/locate/jallcom

Effects of sintering atmosphere on microstructure and electrical properties of $BiScO_3$–$PbTiO_3$ high-temperature piezoceramics

Zeyong Cai, Genshui Wang*, Gang Yu, Zhen Huang, Fei Cao, Xianlin Dong

Key Laboratory of Inorganic Functional Materials and Devices, Shanghai Institute of Ceramics, Chinese Academy of Sciences, 1295 Dingxi Road, Shanghai 200050, People's Republic of China

ARTICLE INFO

Article history:
Received 19 November 2011
Received in revised form 8 February 2012
Accepted 13 February 2012
Available online xxx

Keywords:
Piezoelectric ceramics
High temperature applications
Sintering atomosphere

ABSTRACT

$BiScO_3$–$PbTiO_3$ piezoelectric ceramics were fabricated by the conventional solid state reaction method. The effects of sintering atmosphere on microstructure and electrical properties of $BiScO_3$–$PbTiO_3$ were studied. Different weight changes were found in samples sintered in different atmospheres. X-ray diffraction analysis reveals that all the samples have perovskite structure and a second phase is observed in the samples sintered in sacrificial powders. EDS analysis suggests the second phase could be the compound containing Bi and Pb. Samples sintered in air show lower dielectric constant than those sintered in sacrificial powders, but a higher piezoelectric coefficient. The resisitivity of samples sintered in air is about one order of magnitude higher than that of those sintered in sacrificial powders. These results suggest a promising method to gain $BiScO_3$–$PbTiO_3$ high-temperature piezoceramics with excellent electromechanical properties.

1. Introduction

High-temperature piezoelectric sensors are important to deep oil drilling, space exploration and land-based turbine technology [1,2]. The traditional piezoelectric materials for high-temperature applications are $Pb(Zr,Ti)O_3$-based ceramics whose Curie temperature is about 360 °C, with piezoelectric constant d_{33} of about 370 pC/N. However, the operating temperature of these ceramics is limited to around 180 °C which is much lower than 300 °C required in the practical applications [1]. Recently, great efforts have been devoted to synthesizing various $Bi(Me)O_3$–$PbTiO_3$ solid solutions for enhancing high T_c ceramics [3]. Especially, the high Curie temperature (around 450 °C) and excellent piezoelectric properties (d_{33} = 460 pC/N) of $BiScO_3$–$PbTiO_3$ system make this kind of material a promising candidate for high-temperature applications [3–7].

Recent studies were mostly focused on improving the electrical properties of $BiScO_3$-based solid solutions through various strategies, such as fabricating fine-grain ceramics [8], creating excess PbO or Bi_2O_3 [9] and doping some agents [10–12]. In these studies, in order to minimize the loss of Pb and Bi during sintering process, all samples were sintered in sealed crucibles filled with sacrificial powders. Obviously, $BiScO_3$–$PbTiO_3$ samples sintered in air resulted in Pb-, Bi-vacancy as well as oxygen-vacancy due to the evaporation of PbO and Bi_2O_3, allowing for the possible displaying of donor-doping and accepter-doping property simultaneously on the as-prepared products. However, there is still limited research concentrating on the effects of sintering atmosphere on the piezoelectric property of $BiScO_3$–$PbTiO_3$ materials.

In the present work, we have prepared $37Bi_{(1+x)}ScO_3$–$63Pb_{(1+x)}TiO_3$ (x = 0, 0.002) ceramics by oxide-mixed method. The samples were sintered in different atmospheres. The effects of sintering atmospheres on the microstructure and electrical properties of these ceramics have been systematically investigated. We found that samples sintered in air result in good properties for high-temperature piezoelectric applications.

2. Experimental procedure

2.1. Sample preparation

$37Bi_{(1+x)}ScO_3$–$63Pb_{(1+x)}TiO_3$ (x = 0, 0.002) ceramics (denoted as BSPT-0 and BSPT-0.002, respectively) were prepared through the conventional solid-state synthesis. The starting powders were Bi_2O_3 of 99.9% purity, Sc_2O_3 of 99.46% purity, PbO of 97.39% purity, and TiO_2 of 99.38% purity. The powders were milled with stabilized zircania media for 24 h, and dried at 120 °C. The dried powders were calcined at 750 °C for 6 h, and then ball milled again for 24 h. After drying, 6 wt% PVA was mixed into the powders. The mixture was pressed into pellets of 14 mm in diameter and 2 mm in thickness at 200 MPa. Disk shaped samples were heated to 800 °C for 1 h to remove the binder, and some of them were placed into a sealed Al_2O_3 crucible and sintered for 1.5 h, and then crushed for sacrificial powders. The others of the after burnt-out pieces were sintered in sealed crucibles with the sacrificial powders or sintered in air at 1050–1100 °C for 1–2 h. The samples sintered in air were put on Al_2O_3 panel exposed in furnace. In this work, the samples were prepared in below conditions: (1) BSPT-0.002 pieces were sintered in BSPT-0.002 sacrificial powders, denoted as S11; (2) BSPT-0.002 pieces were

* Corresponding author. Tel.: +86 21 52411123; fax: +86 21 52411104.
E-mail address: genshuiwang@mail.sic.ac.cn (G. Wang).

0925-8388/$ – see front matter © 2012 Elsevier B.V. All rights reserved.
doi:10.1016/j.jallcom.2012.02.092

Table 1
Detailed weight change and density, dielectric relaxor characteristic, piezoelectric and dielectric properties of BSPT ceramics sintered in different atmospheres.

Sample	Weight change during sintering	Density	T_m (°C) (1 kHz)	ΔT_m (°C)	γ	Dielectric constant (1 kHz)	Loss tangent (1 kHz)	Piezoelectric coefficient, d_{33} (pC/N)
S11	0.019%	7.478	435	8	1.70	1138	0.05	229
S13	−0.808%	7.441	422	9	1.68	1039	0.042	361
S21	0.020%	7.491	430	9	1.70	1185	0.039	259
S23	−0.709%	7.424	423	9	1.87	1084	0.045	370

sintered in air, denoted as S13; (3) BSPT-0 pieces were sintered in BSPT-0 sacrificial powders, denoted as S21; (4) BSPT-0 pieces were sintered in air, denoted as S23.

The bulk density was measured by the Archimedes method and the weight change was measured by electronic balance (an accuracy of 10^{-4} g). All samples achieved >95% of theoretical density. The detailed weight change and the density were listed in Table 1.

2.2. Sample characterization

X-ray diffraction (XRD) was performed using an automated diffractometer (Model Rigaku RAX-10 D/max 2550v, Rigaku Co., Tokyo, Japan) with Cu $k\alpha$ radiation operated at room temperature to determine phase assemblage. The microstructures and atom ratios of the ceramic samples were observed using electron probe X-ray microanalyzer (EPMA; JXA-8100, JEOL, Japan). The samples for electron probe X-ray microanalyzer (EPMA) were polished, cleaned, and then acid etched in a mixture of hydrofluoric acid and muriatic acid for several seconds. For electrical measurements, the sintered samples were electroded by a silver paste and pooled in an oil bath under a field of 40 kV/cm at 100 °C for 15 min. The piezoelectric constant was measured using a d_{33} meter (Model ZJ-3D, Institute of Acoustics, Beijing, China). The temperature dependence of the dielectric constants and losses was measured at different frequencies using a Precision LCR Meter (Agilent, 4284A, HP) connected to a high-temperature tube furnace. The ferroelectric *P–E* hysteresis loops were measured using a ferroelectric hysteresis measurement tester (TF analyzer 2000) at room temperature at 10 Hz. An applying voltage of 50 V and a holding time of 1 min were adopted to measure the resistivity using a high resistance meter (HP4329A, Hewlett-Packard, CA).

3. Results and discussion

3.1. Phase structure and microstructure

All samples reveal different weight change (Table 1). The weight change differences between these samples can be attributed to the different sintering atmospheres. As presented in Fig. 1, there is uniquely perovskite phase in the samples sintered in air, however, besides perovskite phase, impurity phase is observed in samples sintered in sacrificial powders. We can reasonably infer that the impurity phase is formed by the Pb (and Bi) diffusion which may result from high Pb (and Bi) sintering atmosphere. This impurity phase will be discussed later.

Fig. 2 shows the EPMA micrographs of a polished surface for BSPT ceramics. Thick grain boundaries are obviously observed for

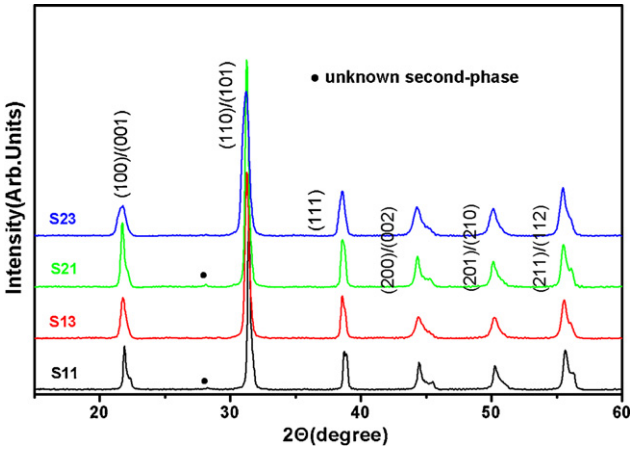

Fig. 1. XRD patterns of BSPT ceramics of different sintering atmospheres.

samples sintered in sacrificial powders. This thick grain boundary could be attributed to the chemical etching of second-phase enriched in grain boundaries. But samples sintered in air show thin grain boundaries, indicating less or no second-phase, which is consistent with the performance of the XRD. Atom ratios from the etching surface containing a region of grains and grain boundaries by EDS are summarized in Table 2. Bi/Sc ratio of samples sintered in sacrificial powders is far less than the nominal ratio of 1, while samples sintered in air possess a Bi/Sc ratio more close to 1. Pb/Ti ratios of all samples are below the nominal ratio of 1. In addition, the Ti/(Ti + Sc) ratios of samples sintered in sacrificial powders are less than the nominal ratio of 0.63. Despite the low accuracy of EDS (±5%), the large shift of Bi/Sc and Pb/Ti ratios from the nominal ratios effectively suggests that grains of all samples sintered in sacrificial powders are Bi-, Pb-deficient. As discussed above, it can be reasonably inferred that the second-phase eroded by acids may contain Bi and Pb. Grains of samples sintered in air have higher Bi content than those sintered in sacrificial powders, and the higher Bi content results in higher piezoelectric coefficient, which is consistent with the previous work [9].

3.2. Electrical characterization

Fig. 3 shows the temperature dependence of dielectric constant under five different frequencies (10^2, 10^3, 10^4, 10^5, 10^6 Hz). The dielectric peaks of all samples obviously change when the frequency increases. This behavior is the typical characteristic of relaxor ferroelectrics. The dielectric characteristics of relaxor ferroelectrics are known to deviate from the typical Curie–Weiss behavior and can be described by a modified Curie–Weiss relationship [13,14]:

$$\frac{1}{\varepsilon_r} - \frac{1}{\varepsilon_{rm}} = \frac{(T - T_m)^\gamma}{C}, \quad 1 \le \gamma \le 2 \tag{1}$$

where ε_{rm} is the maximum value of the dielectric constant at the transition temperature T_m, C is the Curie-like constant, and γ is the degree of diffuseness where the value of γ varies between 1 and 2. The value $\gamma = 1$ corresponds to a normal ferroelectric and $\gamma = 2$ is applicable to an ideal relaxor ferroelectric [15]. The inset in Fig. 3 shows the plot of $\ln(\varepsilon_r - \varepsilon_{rm})$ versus $\ln(T - T_m)$ of samples at 1 MHz. The curves can be fit to Eq. (1) showing that all samples exhibit a highly linear relation with high degree of diffuseness (Table 1), which exemplifies a typical relaxor behavior. The frequency dispersion data are summarized in Table 1, where ΔT_m is the T_m difference between 100 Hz and 1 MHz.

According to previous studies [16–18], it is considered that in the mixed B-site family the relaxor behavior in ferroelectric materials

Table 2
Atom ratios of BSPT ceramics of different sintering atmosphere.

Sample	Bi/Sc	Pb/Ti	Bi/(Bi + Pb)	Ti/(Sc + Ti)
S11	0.8051	0.8066	0.3729	0.6267
S13	0.9671	0.7694	0.4096	0.6444
S21	0.8149	0.7866	0.3951	0.6133
S23	0.8713	0.7821	0.3869	0.6384

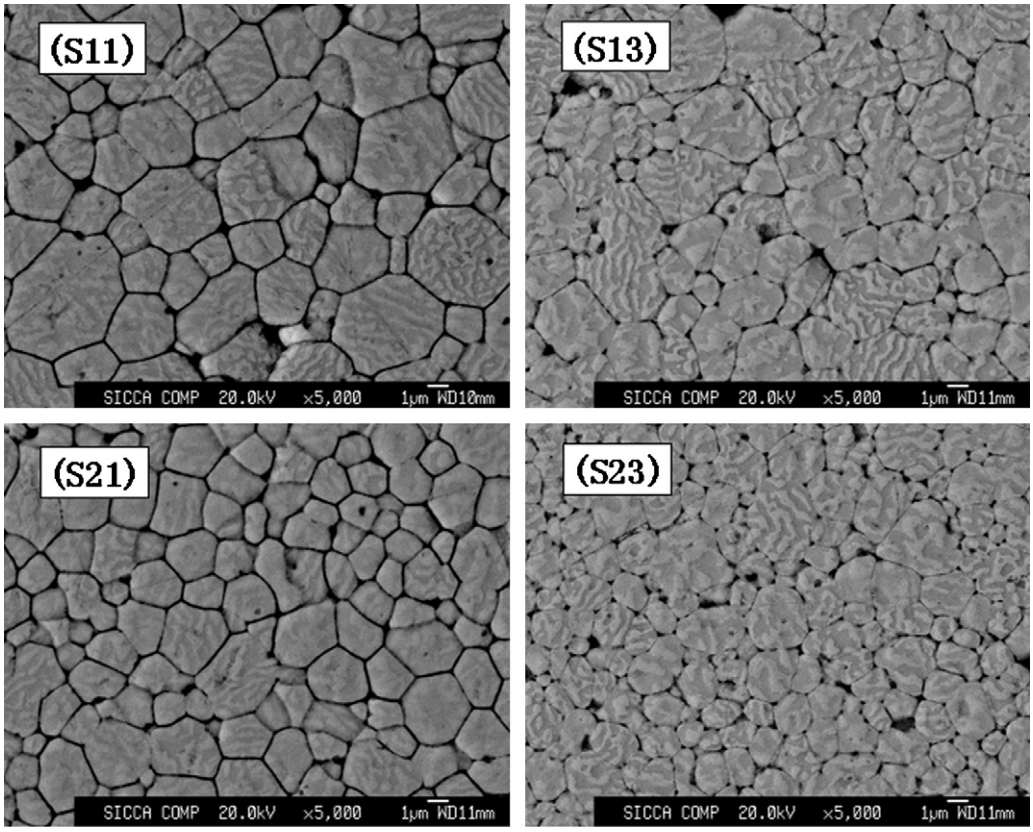

Fig. 2. EPMA micrographs of polished surface of BSPT ceramics of different sintering atmospheres.

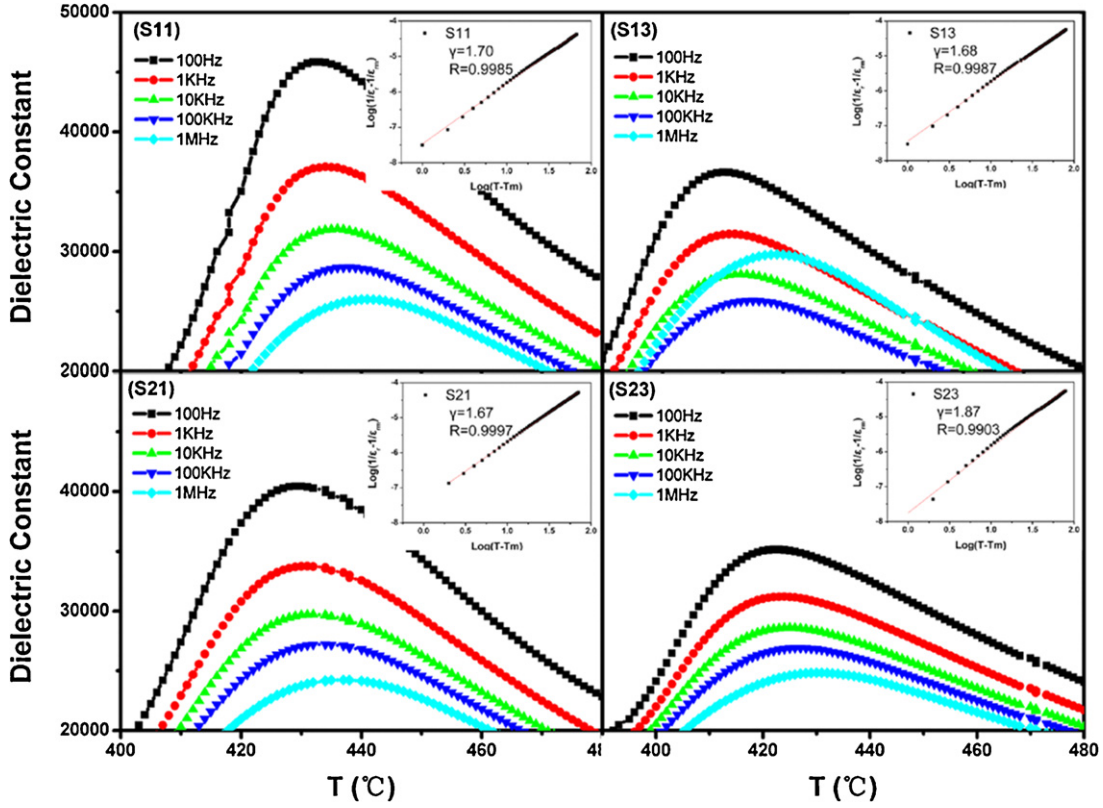

Fig. 3. Temperature dependence of dielectric constant of BSPT ceramics of different sintering atmospheres. The inset shows plots of $\log((1/\varepsilon_r)-(1/\varepsilon_{rm}))$ versus $\log(T-T_m)$ for BSPT of different sintering atmospheres at 1 MHz. γ and R represent respectively the degree of diffuseness and degree of fitting.

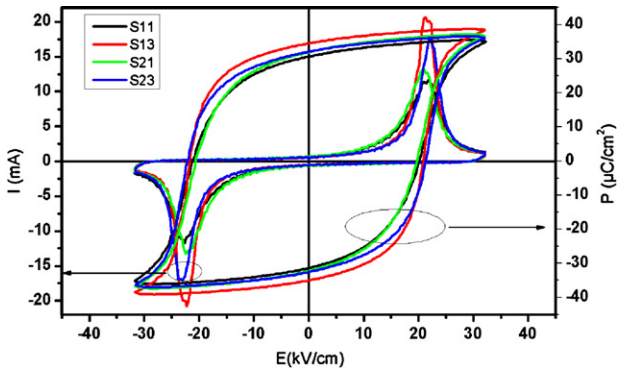

Fig. 4. *I–E* and *P–E* curves of BSPT ceramics of different sintering atmospheres.

came from the local heterogeneity due to the different ions possessing fluctuating valence states at the B site. For $BiScO_3$–$PbTiO_3$ system, mutual substitution of Sc^{3+} and Ti^{4+} or Bi^{3+} and Pb^{2+} can lead to a local disorder at the B site and the disruption of a long-range order, which may lead to the relaxation.

Table 1 shows the piezoelectric and dielectric properties of samples sintered in different atmospheres. All samples show mixed phase and similar dielectric loss. The T_m of the S13 sample is 13 °C, lower than that of S11, but S13 samples have an enhanced piezoelectric coefficient. This trend is also observed for the S21 and S23 samples.

The polarization–electrical field (*P–E*) and current–electrical field (*I–E*) hysteresis loop for samples of different sintering atmospheres were measured at room temperature at 10 Hz. Fig. 4 shows the *I–E* and the *P–E* curves. Higher peaks current of S13 and S23 are observed, indicating more domain walls switching under coercive field, which is consistent with the observation of higher piezoelectric coefficient of S13 and S23. All samples show square hysteresis loops as a result of A-site vacancies effect which was proposed by Sehirlioglu et al. [19]. This is consistent with the observation of EDS which indicated that all grains were of Bi-, Pb-deficiency.

Fig. 5 shows the DC resistivity of the BSPT sintered in different atmospheres. It was found that the resisitivity of samples sintered in air is higher than that of those sintered in sacrificial powders throughout the whole temperature range studied. The lower resistivity of sample sintered in sacrificial powders may be attributed to the second-phase at grain-boundary which would cause the decrease in resistance [20]. The resistivity of both samples sintered in air is more than 10^9 Ω cm at 400 °C. The temperature dependence of conductivity was fitted according to the Arrhenius equation:

$$\rho = A \exp\left(\frac{E_a}{kT}\right) \quad (2)$$

where E_a is the nominal activation energy per charge carriers, k is Boltzmann's constant, and T is the temperature. From Eq. (2), it can be seen that $\ln \rho$ has a linear relationship with $1/T$ and the E_a can be determined in terms of the slope of the Arrhenius plots. The fitted results were shown in Fig. 5. From the Arrhenius plots, the values of E_a of each regions of the slope on the heating run were calculated. There are two regions predominant with different conduction mechanisms. At the low temperature region, the activation energy of all samples was about 0.24 eV, which may be due to extrinsic conduction of the short-range diffusion and the rearrangement of oxygen vacancies [21]. At the high temperature range, the activation energies were in the range of 1.32–2.02 eV for all samples, which were ascribed to the polycrystalline nature of the materials [22]. The intrinsic electronic conductivity activation energy is equal to half the energy of the band gap E_g; therefore, the band gap of BSPT is about 3.4 eV. This value fits well with that of $BaTiO_3$ (about 3.3 eV), and the similarity of the band gap is due to

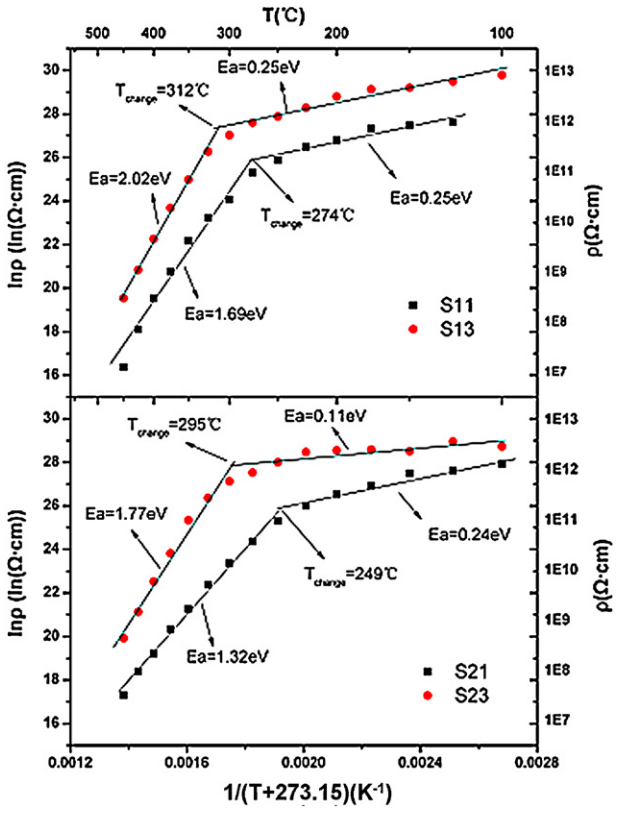

Fig. 5. Temperature dependence of resistivity of BSPT ceramics sintered in different atmospheres.

the common TiO_6 octahedra [23]. Fig. 5 also shows that the temperature corresponding to transformation from extrinsic to intrinsic range increased when samples were sintered in air. The conduction mechanism of BSPT should be studied further.

4. Conclusion

Effects of sintering atmosphere on microstructure and electrical properties of BSPT piezoceramics have been investigated. Compared to the samples sintered in sacrificial powders, the samples sintered in air showed a higher piezoelectric constant and a lower Curie temperature. Samples sintered in air exhibited single perovskite phase while samples sintered in sacrificial powders had minor Bi-, Pb-contained second-phase besides perovskite phase. All samples showed typical relaxor characteristic which might be explained by mutual substitution of Sc^{3+} and Ti^{4+} or Pb^{2+} and Bi^{3+}. *P–E* curves show that all samples are donor-doping characteristic (A-site vacancies). Samples sintered in air revealed higher resistivity than those sintered in sacrificial powders. These results suggested that samples sintered in air may be a promising material for high-temperature applications.

Acknowledgment

This work was supported by National High Technology Research and Development Program (863 program) of China (2009AA03Z108) Shanghai Basic Research Project (No. 10DJ1400203).

References

[1] R. Turner, P. Fuierer, R. Newnham, T. Shrout, Appl. Acoust. 41 (1994) 299–324.

[2] D. Damjanovic, Curr. Opin. Solid State Mater. Sci. 3 (1998) 469–473.
[3] R.E. Eitel, C.A. Randall, T.R. Shrout, P.W. Rehrig, W. Hackenberger, S.E. Park, Jpn. J. Appl. Phys. 40 (2001) 5999.
[4] R.E. Eitel, C.A. Randall, T.R. Shrout, S.E. Park, Jpn. J. Appl. Phys. 41 (2002) 2099.
[5] C.A. Randall, R.E. Eitel, T.R. Shrout, D. Woodward, I. Reaney, J. Appl. Phys. 93 (2003) 9271.
[6] S. Zhang, C.A. Randall, T.R. Shrout, Appl. Phys. Lett. 83 (2003) 3150.
[7] R. Eitel, S. Zhang, T. Shrout, C. Randall, I. Levin, J. Appl. Phys. 96 (2004) 2828.
[8] T.T. Zou, X.H. Wang, L.T. Li, Key Eng. Mater. 368 (2008) 8–10.
[9] A. Sehirlioglu, A. Sayir, F. Dynys, J. Appl. Phys. 106 (2009), 014102-02-7.
[10] R.E. Eitel, T.R. Shrout, C.A. Randall, Jpn. J. Appl. Phys. 43 (2004) 8146.
[11] P. Winotai, N. Udomkan, S. Meejoo, Sens. Actuators A: Phys. 122 (2005) 257–263.
[12] S. Zhang, R.E. Eitel, C.A. Randall, T.R. Shrout, E.F. Alberta, Appl. Phys. Lett. 86 (2005), 262904-04-3.
[13] W.J. Merz, Phys. Rev. 91 (1953) 513.
[14] H. Martirena, J. Burfoot, Ferroelectrics 7 (1974) 151–152.
[15] K. Uchino, S. Nomura, Ferroelectrics 44 (1982) 55–61.
[16] V. Isupov, Sov. Phys. Tech. Phys. 1 (1956) 1846.
[17] B.N. Rolov, Sov. Phys. Solid State 6 (1965) 1676.
[18] G. Smolenskii, J. Phys. Soc. Jpn. 28 (1970) 26–37.
[19] A. Sehirlioglu, A. Sayir, F. Dynys, J. Am. Ceram. Soc. 93 (2010) 1718–1724.
[20] A. Sehirlioglu, A. Sayir, F. Dynys, J. Am. Ceram. Soc. 91 (2008) 2910–2916.
[21] M.M. Ahmad, K. Yamada, Appl. Phys. Lett. 90 (2007) 112902.
[22] K. Srinivas, A.R. James, J. Appl. Phys. 86 (1999) 3885.
[23] S. Ehara, K. Muramatsu, M. Shimazu, J. Tanaka, M.I. Tsukioka, Y. Mori, Jpn. J. Appl. Phys. 20 (1981) 877.